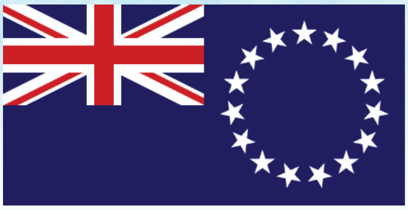

Chapter 2

Cook Islands

2.1 Climate Summary

2.1.1 Current Climate

- Warming trends are evident in annual and half-year maximum and minimum air temperatures at Rarotonga (Southern Cook Islands) for the period 1934–2011. For the period 1941–1991 there was no trend in annual mean temperature at Penrhyn (Northern Cook Islands).
- The annual number of Warm Days and Warm Nights from 1935 increased at Rarotonga, while the number of Cold Nights has decreased.
- Annual and half-year rainfall trends show little change at Rarotonga since 1899 and Penrhyn since 1937. There has also been little change in extreme daily rainfall at both sites since the mid 1930s.
- Tropical cyclones affect the Cook Islands mainly between November and April. An average of 18 cyclones per decade developed within or crossed the Cook Islands Exclusive Economic Zone (EEZ) between the 1969/70 and 2010/11 seasons. Tropical cyclones were most frequent in El Niño years (28 cyclones per decade) and least frequent in La Niña years (6 cyclones per decade). Seventeen of the 53 tropical cyclones (32%) between the 1981/82 and 2010/11 seasons became severe events (Category 3 or higher) within the Cook Islands EEZ. Available data are not suitable for assessing long-term trends.
- Wind-waves in the Cook Islands are dominated by trade winds and the South Pacific Convergence Zone (SPCZ) seasonally, and the El Niño–Southern Oscillation (ENSO) and Southern Annular Mode (SAM) interannually. Larger storm waves are seen in the Southern Cook Islands than in the Northern Cook Islands. Available data are not suitable for assessing long-term trends (see Section 1.3).

2.1.2 Climate Projections

For the period to 2100, the latest global climate model (GCM) projections and climate science findings indicate:

- El Niño and La Niña events will continue to occur in the future (*very high confidence*), but there is little consensus on whether these events will change in intensity or frequency;
- Annual mean temperatures and extremely high daily temperatures will continue to rise (*very high confidence*);
- Average annual rainfall is projected to stay similar to the current climate, except for a small decrease in May–October in the Northern Cook Islands under the high emission scenario (*medium confidence*), with more extreme rain events (*high confidence*);
- Drought frequency is projected to remain similar to the current climate in the Southern Cook Islands, but increase slightly in the Northern Cook Islands under the high emission scenario (*medium confidence*);
- Ocean acidification is expected to continue *(very high confidence)*;
- The risk of coral bleaching is expected to increase (*very high confidence)*;
- Sea level will continue to rise *(very high confidence)*; and
- Wave climate is not projected to change significantly *(low confidence)*.

2.2 Data Availability

The Cook Islands Meteorological Service is responsible for monitoring weather and climate in the Cook Islands. It currently operates six automatic weather stations on three of the Southern Cook Islands (Mangaia, Mauke, Aitutaki) and three of the Northern Cook Islands (Pukapuka, Penrhyn, Manihiki). Good quality historical manually observed meteorological data exist for six stations until the mid-1990s. Observations are sporadic after this period, with the exception of Rarotonga the main observation station where manual multiple 24-hr observations continue to present day. The Rarotonga climate station is located at Nikao, near the western end of the Rarotonga International Airport runway, on the north-western side of the island. Data are available here from 1899 to present for rainfall and from 1907 to present for air temperature. For Penrhyn, rainfall data are available from 1937 to present, and air temperature data from 1941 to 1995. The Penrhyn rainfall record from October 1996 has been constructed from Cook Islands Meteorological Service AWS data and manual observations from two other sites on the island. Temperature data from the AWS have not been used due to quality issues.

Rarotonga rainfall from 1899 (daily values from 1937) and air temperature data from 1934, as well as Penrhyn rainfall from 1937 and air temperature data from 1941 to 1991, have been used in this report. Both records are homogeneous. Additional information on historical climate trends in the Cook Islands region can be found in the Pacific Climate Change Data Portal www.bom.gov.au/climate/pccsp/.

Wind-wave data from buoys are particularly sparse in the Pacific region, with very short records. Model and reanalysis data are therefore required to detail the wind-wave climate of the region. Reanalysis surface wind data have been used to drive a wave model over the period 1979–2009 to generate a hindcast of the historical wind-wave climate.

2.3 Seasonal Cycles

Information on temperature and rainfall seasonal cycles can be found in Australian Bureau of Meteorology and CSIRO (2011).

2.3.1 Wind-driven Waves

The wind-wave climate of the Cook Islands shows differences between the Northern Cook Islands and the Southern Cook Islands.

In the Southern Cook Islands (e.g. on the north coast of Rarotonga), waves are predominantly driven by trade winds, showing strong seasonal variability of direction with a rotation from the southeast in June–September to the northeast during December–March (Figure 2.1). There is no significant variation in wave height or period throughout the year (Table 2.1), though monthly mean periods are slightly longer during December–March (mean around 9.8 s) than during June–September (mean around 9.0 s). The wave climate is characterised by trade wind generated waves from the east, and a small component of swell propagated from storm events in the Southern Ocean throughout the year and also from the north during December–March due to Northern Hemisphere storms and tropical depressions. Waves larger than 3.4 m (99th percentile) at Rarotonga occur predominantly during December–March. They are usually directed from the north, associated with cyclones and North Pacific storm swell, with some large south-easterly and westerly waves observed during June–September, associated with Southern Ocean storms. The height of a 1-in-50 year wave event on the north coast of Rarotonga is calculated to be 11.1 m.

In the Northern Cook Islands (e.g. on the west coast of Penrhyn), waves are characterised by variability of trade winds and location of the South Pacific Convergence Zone (SPCZ). Trade winds generate local waves from the northeast, though south-easterly waves may be blocked at this location by the island (Figure 2.2). Wave height and period remain fairly constant throughout the year (Table 2.1). In December–March waves are on average north-westerly; comprising some locally generated north-easterly waves, with north-westerly swell waves from cyclones and North Pacific storms, and some south-westerly swell. In June–September, waves are predominantly from the south-southwest, propagating as swell from southern mid-latitude storm events, with a smaller proportion of the wave field being locally generated north-easterly waves. Waves larger than 2.8 m (99th percentile) occur predominantly during December–March from the west-northwest due to tropical cyclones, with some large southerly waves during June–September from extra-tropical storms. The height of a 1-in-50 year wave event on the west coast of Penrhyn is calculated to be 6.8 m.

No suitable dataset is available to assess long-term historical trends in the Cook Islands wave climate. However, interannual variability may be assessed in the hindcast record. The wind-wave climate displays strong interannual variability in the Cook Islands, varying with the El Niño–Southern Oscillation (ENSO) and the Southern Annular Mode (SAM). During La Niña years, wave power on the west coast of Penrhyn is less than during El Niño years, and waves are less strongly directed from the west, associated with increased trade wind speeds. At Rarotonga, in December–March waves have slightly more power in El Niño years though less than at Penrhyn, while in June–September waves have approximately 30% more power in La Niña years and are more strongly directed from the east, associated with a strengthening of southern trade winds and movement of the SPCZ. When the SAM index is negative, waves at Rarotonga are directed less strongly from the east, while waves at Penrhyn are directed slightly more strongly from the west, associated with increased westerly swell due to enhanced mid-latitude storms in the Southern Ocean.

Table 2.1: Mean wave height, period and direction from which the waves are travelling around the Cook Islands in December–March (wet season) and June–September (dry season). Observation (hindcast) and climate model simulation mean values are given for the Northern and Southern Cook Islands with the 5–95th percentile range (in brackets). Historical model simulation values are given for comparison with projections (see Section 2.5.6 and Tables 2.9 and 2.10). A compass relating number of degrees to cardinal points (direction) is shown.

		**Hindcast Reference Data (1979–2009) north Rarotonga (Southern Cook Islands)**	**Climate Model Simulations (1986–2005) (Southern Cook Islands)**	**Hindcast Reference Data (1979–2009) west Penrhyn (Northern Cook Islands)**	**Climate Model Simulations (1986–2005) (Northern Cook Islands)**
Wave Height (metres)	December–March	1.8 (1.2–2.7m)	2.0 (1.6–2.4m)	1.7 (1.2–2.4m)	1.9 (1.5–2.3m)
	June–September	1.7 (1.1–2.6)	2.2 (1.8–2.7)	1.6 (1.1–2.2)	1.9 (1.6–2.2)
Wave Period (seconds)	December–March	9.8 (7.5–12.7)	9.4 (7.8–11.0)	11.1 (8.6–13.9)	10.1 (8.3–11.9)
	June–September	9.0 (6.9–11.8)	9.0 (8.0–10.1)	10.5 (7.9–13.5)	8.5 (7.3–9.8)
Wave Direction (degrees clockwise from North)	December–March	30 (280–130°)	90 (10–160°)	340 (200–70°)	20 (330–70°)
	June–September	150 (70–240°)	160 (140–200°)	170 (110–210°)	140 (120–150°)

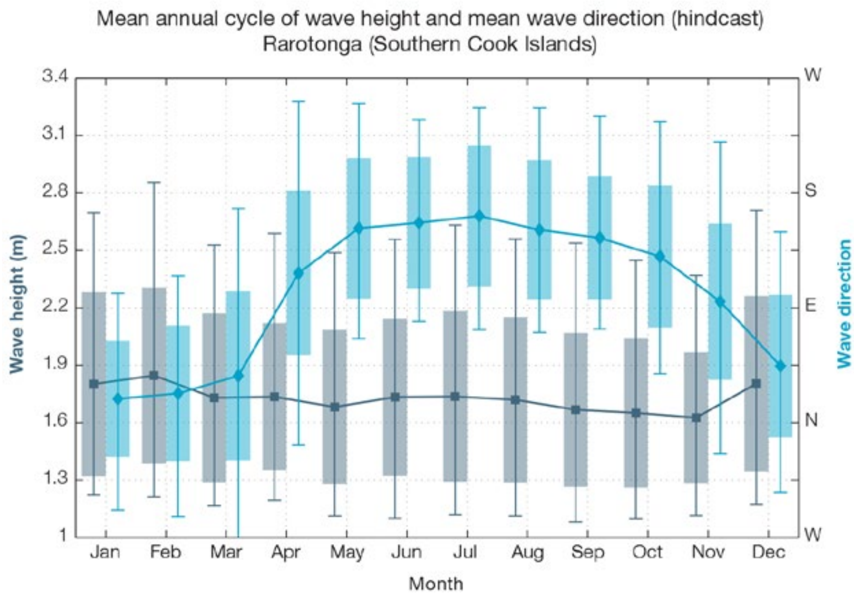

Figure 2.1: Mean annual cycle of wave height (grey) and mean wave direction (blue) at Rarotonga (Southern Cook Islands) in hindcast data (1979–2009). To give an indication of interannual variability of the monthly means of the hindcast data, shaded boxes show 1 standard deviation around the monthly means, and error bars show the 5–95% range. The direction from which the waves are travelling is shown (not the direction towards which they are travelling).

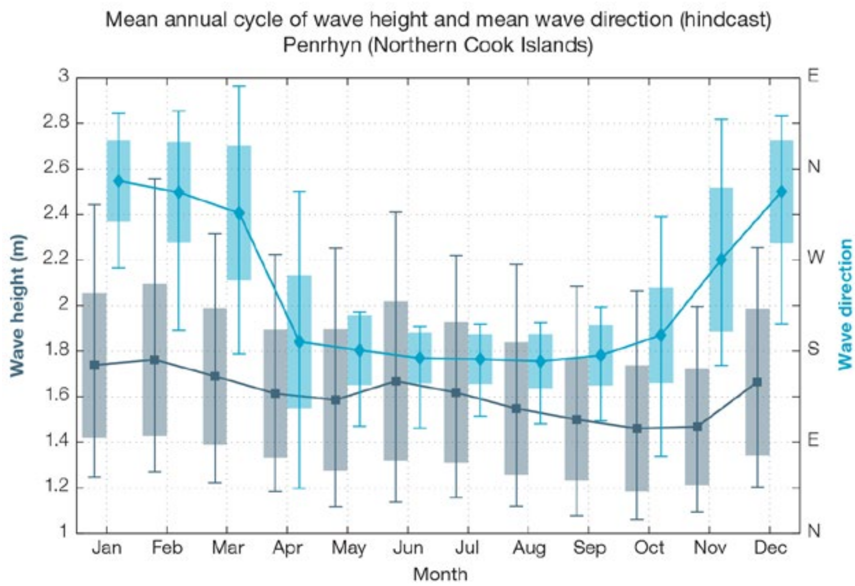

Figure 2.2: Mean annual cycle of wave height (grey) and mean wave direction (blue) at Penrhyn (Northern Cook Islands) in hindcast data (1979–2009). To give an indication of interannual variability of the monthly means of the hindcast data, shaded boxes show 1 standard deviation around the monthly means, and error bars show the 5–95% range. The direction from which the waves are travelling is shown (not the direction towards which they are travelling).

2.4 Observed Trends

2.4.1 Air Temperature

Annual and Half-year Mean Air Temperature

Warming trends (Figure 2.3 and Table 2.2) of similar magnitude have been identified in annual, May–October, and November–April mean air temperatures at Rarotonga for the 1934–2011 period. Annual and half-year minimum air temperature trends are greater than those observed for maximum air temperatures at Rarotonga (Table 2.2). Over the period 1941–1991, the annual, winter and summer Rarotonga trends are slightly larger and more significant compared to Penrhyn (Figure 2.4) over the same period. This suggests that the warming at Penrhyn is slightly less than we see at Rarotonga.

Extreme Daily Air Temperature

Warming trends are also evident in the extreme indices (Table 2.3). The annual number of Warm Day and Warm Nights has increased at Rarotonga, while the number of Cold Nights has decreased (Figure 2.5). These trends are statistically significant at the 5% level and consistent with global warming trends. Trends in extreme temperatures at Penrhyn could not be calculated due to insufficient data.

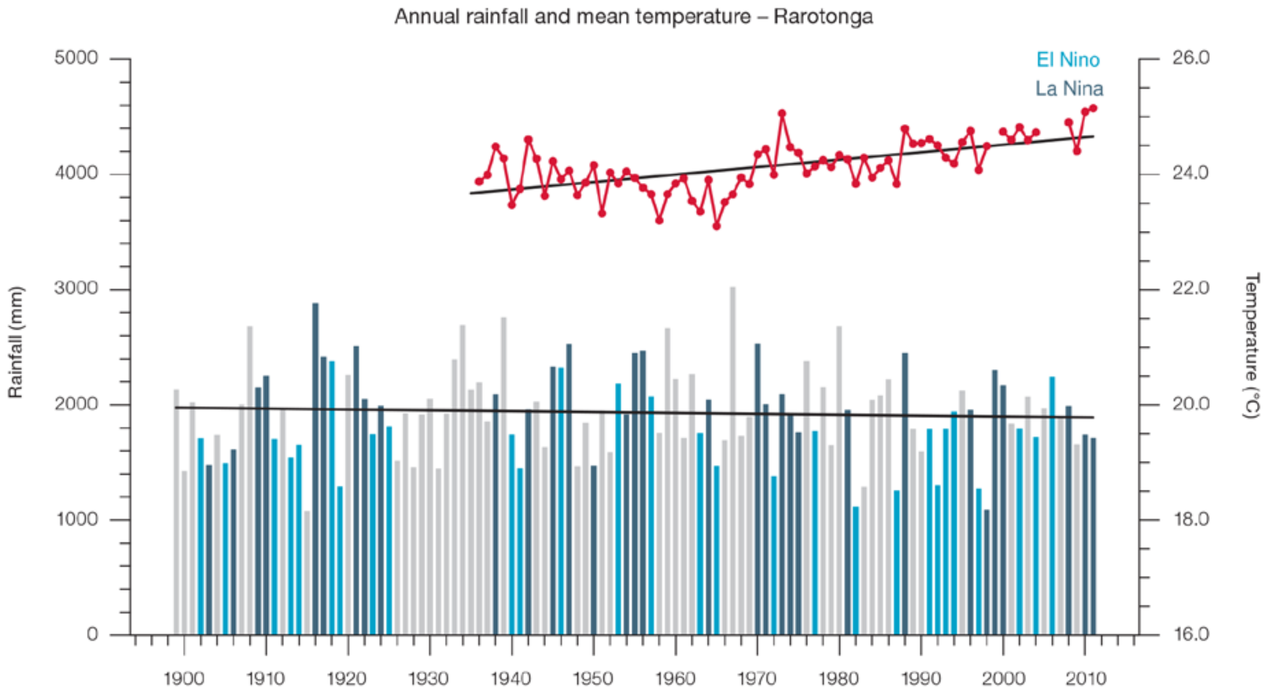

Figure 2.3: Observed time series of annual average values of mean air temperature (red dots and line) and total rainfall (bars) at Rarotonga. Light blue, dark blue and grey bars denote El Niño, La Niña and neutral years respectively. Solid black trend lines indicate a least squares fit.

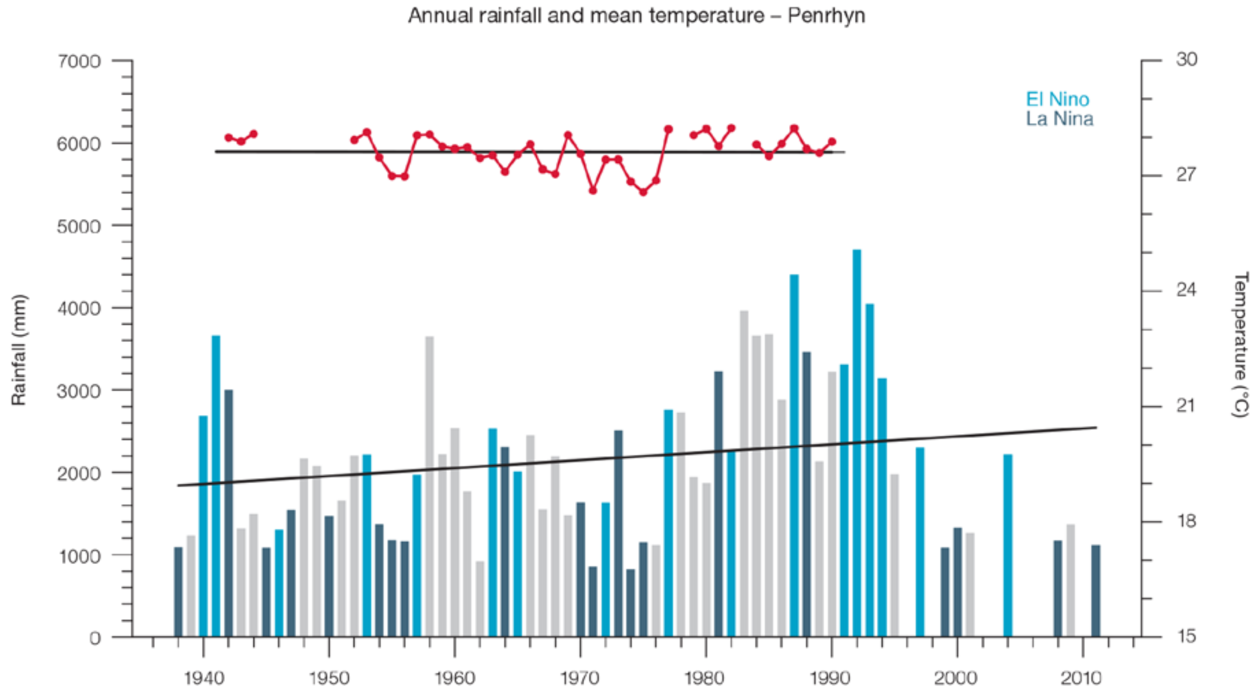

Figure 2.4: Observed time series of annual average values of mean air temperature (red dots and line) and total rainfall (bars) at Penrhyn. Light blue, dark blue and grey bars denote El Niño, La Niña and neutral years respectively. Solid black trend lines indicate a least squares fit.

Table 2.2: Annual, wet season (Nov-Apr) and dry season (May-Oct) trends in air temperature (Tmax, Tmin, Tmean) and rainfall at Rarotonga (top) and Penrhyn (bottom). The 95% confidence intervals are shown in brackets. Values for trends that are significant at the 5% level are shown in **boldface**.

Rarotonga (Southern Cook Islands)	Tmax (°C/10yrs)	Tmin (°C/10yrs) 1934–2011	Tmean (°C/10yrs)	Total Rainfall (mm/10yrs) 1899–2011
Annual	**+0.09** (+0.02, +0.17)	**+0.19** (+0.13, +0.25)	**+0.14** (+0.07, +0.20)	-4.9 (-30.1, +17.4)
Nov–Apr (wet season)	**+0.09** (+0.01, +0.17)	**+0.18** (+0.12, +0.24)	**+0.12** (+0.06, +0.18)	-25.5 (0, -7.3)
May–Oct (dry season)	**+0.12** (+0.05, +0.22)	+0.20 (+0.13, +0.27)	**+0.18** (+0.11, +0.24)	+0.9 (-11.9, +13.1)

Penrhyn (Northern Cook Islands)	Tmax (°C /10yrs)	Tmin (°C/10yrs) 1941–1991	Tmean (°C/10yrs)	Total Rainfall (mm/10yrs) 1937–2011
Annual	0.09 (-0.15, 0.31)	+0.04 (-0.19, +0.25)	+0.05 (-0.20, +0.24)	+131.8 (-87.3, +371.0)
Nov–Apr	+0.14 (-0.15, 0.41)	+0.15 (-0.15, +0.43)	+0.11 (-0.15, +0.35)	+80.8 (-24.4, +196.6)
May–Oct	+0.04 (-0.16, -0.23)	+0.05 (-0.10, +0.15)	+0.04 (-0.13, +0.19)	+20.1 (-59.4, +102.0)

Table 2.3: Annual trends in air temperature and rainfall extremes at Rarotonga (left) and Penrhyn (right). The 95% confidence intervals are shown in brackets. Values for trends that are significant at the 5% level are shown in **boldface**. Dash ('-') indicates trend not calculated due to insufficient data.

	Rarotonga (Southern Cook Islands)	Penrhyn (Northern Cook Islands)
TEMPERATURE	**(1935–2011)**	
Warm Days (days/decade)	**+7.55** (+2.98, +11.35)	-
Warm Nights (days/decade)	**+6.66** (+4.44, +8.55)	-
Cool Days (days/decade)	**-5.83** (-8.53, -3.31)	-
Cool Nights (days/decade)	**-9.02** (-12.41, -5.30)	-
RAINFALL	**(1934–2011)**	**(1937–2011)**
Rain Days ≥ 1 mm (days/decade)	-1.83 (-4.14, +0.14)	+8.60 (-1.12, +16.82)
Very Wet Days (mm/decade)	-3.69 (-29.75, +21.87)	+74.85 (-29.49, +212.01)
Consecutive Dry Days (days/decade)	+0.21 (0, +0.59)	-0.19 (-0.94, +0.36)
Max 1-day rainfall (mm/decade)	+1.76 (-2.56, +5.52)	+3.62 (-7.44, +15.70)

Warm Days: Number of days with maximum temperature greater than the 90th percentile for the base period 1971–2000
Warm Nights: Number of days with minimum temperature greater than the 90th percentile for the base period 1971–2000
Cool Days: Number of days with maximum temperature less than the 10th percentile for the base period 1971–2000
Cool Nights: Number of days with minimum temperature less than the 10th percentile for the base period 1971–2000
Rain Days ≥ 1 mm: Annual count of days where rainfall is greater or equal to 1 mm (0.039 inches)
Very Wet Day rainfall: Amount of rain in a year where daily rainfall is greater than the 95th percentile for the reference period 1971–2000
Consecutive Dry Days: Maximum number of consecutive days in a year with rainfall less than 1 mm (0.039 inches)
Max 1-day rainfall: Annual maximum 1-day rainfall

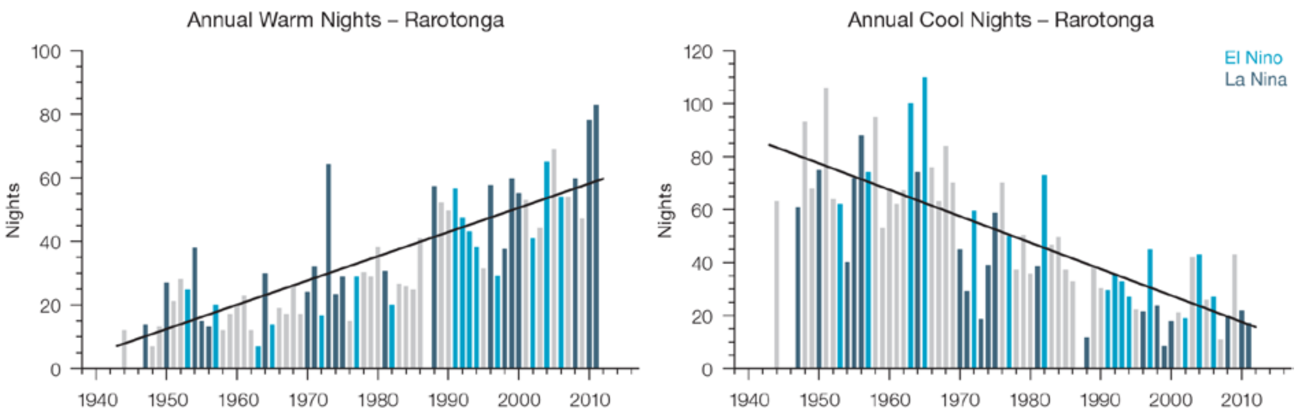

Figure 2.5: Observed time series of annual total number of Warm Nights (left) and Cool Nights (right) at Rarotonga. Solid black trend lines indicate a least squares fit.

2.4.2 Rainfall

Annual and Half-year Total Rainfall

Notable interannual variability associated with ENSO is evident in the observed rainfall records for Rarotonga since 1899 (Figure 2.3) and Penrhyn since 1937 (Figure 2.4). Trends in annual and seasonal rainfall shown in Table 2.2 and Figures 2.3 and 2.4 are not statistically significant at the 5% level. In other words, annual and half-year rainfall trends show little change at Rarotonga and Penrhyn.

Daily Rainfall

Daily rainfall trends for Rarotonga and Penrhyn are also presented in Table 2.3. Due to large year-to-year variability, there are no significant trends in the daily rainfall indices. Figure 2.6 shows statistically insignificant trends in annual Very Wet Days and Rain Days ≥ 1 mm at Rarotonga and Penrhyn.

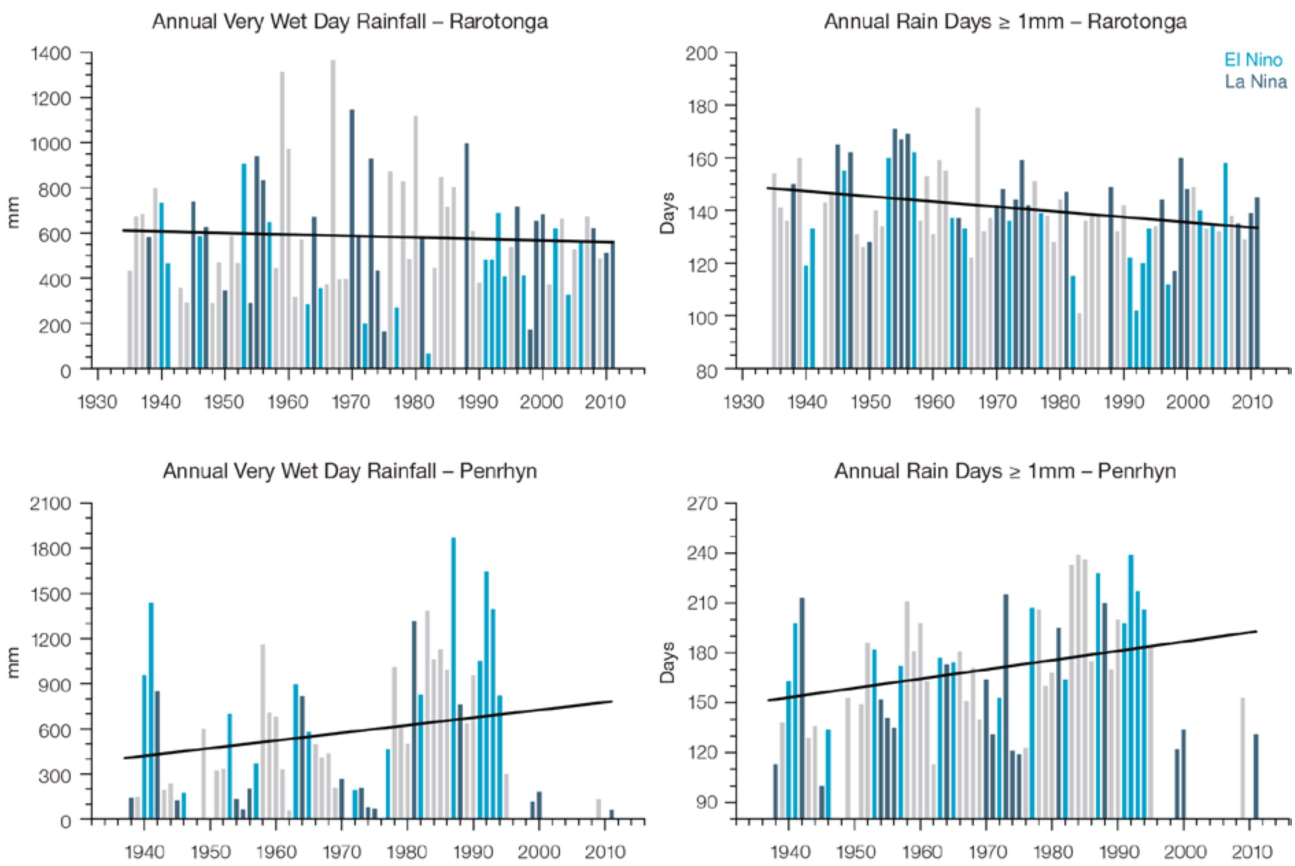

Figure 2.6: Observed time series of annual total values of Very Wet Day rainfall at Rarotonga (top left panel) and Penrhyn (bottom left panel), and annual Rain Days ≥ 1 mm at Rarotonga (top right panel) and Penrhyn (bottom right panel). Solid black line indicates least squares fit.

2.4.3 Tropical Cyclones

When tropical cyclones affect the Cook Islands they tend to do so between November and April. Occurrences outside this period are rare. The tropical cyclone archive for the Southern Hemisphere indicates that between the 1969/70 and 2010/11 seasons, 74 tropical cyclones developed within or crossed the Cook Islands EEZ. This represents an average of 18 cyclones per decade. Refer to Chapter 1, Section 1.4.2 (Tropical Cyclones) for an explanation of the difference in the number of tropical cyclones occurring in the Cook Islands in this report (Australian Bureau of Meteorology and CSIRO, 2014) compared to Australian Bureau of Meteorology and CSIRO (2011).

Interannual variability in the number of tropical cyclones in the Cook Islands EEZ is large, ranging from zero in some seasons to six in the 1980/81, 1997/98 and 2005/06 seasons (Figure 2.7). Tropical cyclones were most frequent in El Niño years (28 cyclones per decade) and least frequent in La Niña years (6 cyclones per decade). The neutral season average is 13 cyclones per decade. Seventeen of the 53 tropical cyclones (32%) between the 1981/82 and 2010/11 seasons became severe events (Category 3 or higher) within the Cook Islands EEZ.

Long-term trends in frequency and intensity have not been presented as country-scale assessment is not recommended. Some tropical cyclone tracks analysed in this subsection include the tropical depression stage (sustained winds less than or equal to 34 knots) before and/or after tropical cyclone formation.

Additional information on historical tropical cyclones in the Cook Islands region can be found at www.bom.gov.au/cyclone/history/tracks/index.shtml

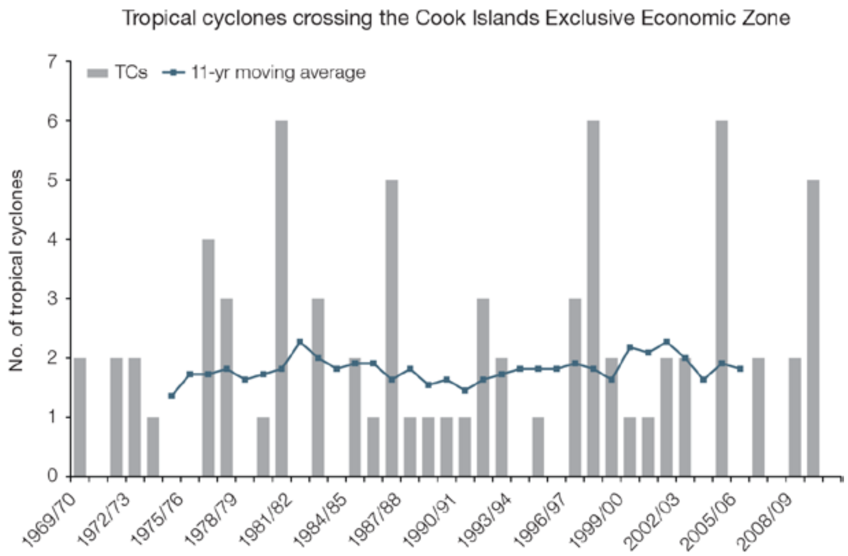

Figure 2.7: Time series of the observed number of tropical cyclones developing within and crossing the Cook Islands EEZ per season. The 11-year moving average is in blue.

2.5 Climate Projections

The performance of the available CMIP5 climate models over the Pacific has been rigorously assessed (Brown et al., 2013a, b; Grose et al., 2014; Widlansky et al., 2013). The simulation of the key processes and features for the Cook Islands region is similar to the previous generation of CMIP3 models, with all the same strengths and many of the same weaknesses. However, the best-performing CMIP5 models used here have lower biases (differences between the simulated and observed climate data) than the best CMIP3 models, and there are fewer poorly-performing models. For the Cook Islands, the most important model bias is that the rainfall maximum of the SPCZ is too zonally (east-west) oriented and therefore the Northern Cook Islands are too wet and the Southern Cook Islands are too dry in models. This lowers confidence in the model projections. Out of 27 models assessed, three models were rejected for use in these projections due to biases in the mean climate and in the simulation of the SPCZ. Climate projections have been derived from up to 24 GCMs in the CMIP5 database (the exact number is different for each scenario, Appendix A), compared with up to 18 models in the CMIP3 database reported in Australian Bureau of Meteorology and CSIRO (2011).

It is important to realise that the models used give different projections under the same scenario. This means there is not a single projected future for the Cook Islands, but rather a range of possible futures for each emission scenario. This range is described below.

2.5.1 Temperature

Further warming is expected over the Cook Islands (Figure 2.8, Tables 2.7 and 2.8). Under all Representative Concentration Pathways (RCPs), the warming is up to 1.0°C by 2030, relative to 1995, but after 2030 there is a growing difference in warming between each RCP. For example, in the Northern Cook Islands by 2090, a warming of 2.0 to 3.8°C is projected for RCP8.5 (very high emissions) while a warming of 0.5 to 1.2°C is projected for RCP2.6 (very low emissions). The total range of projected temperatures is broader than that presented in Australian Bureau of Meteorology and CSIRO (2011) because a wider range of emissions scenarios is considered. While relatively warm and cool years and decades will still occur due to natural variability, there is projected to be more warm years and decades on average in a warmer climate.

There is *very high confidence* that temperatures will rise because:

- It is known from theory and observations that an increase in greenhouse gases will lead to a warming of the atmosphere; and
- Climate models agree that the long-term average temperature will rise.

There is *medium confidence* in the model average temperature change shown in Tables 2.7 and 2.8 because:

- The new models simulate the rate of temperature change of the recent past with reasonable accuracy; and
- There are biases in the simulation of sea-surface temperatures in the region of the Cook Islands, and associated biases in the simulation of the SPCZ, which affect projections of both temperature and rainfall.

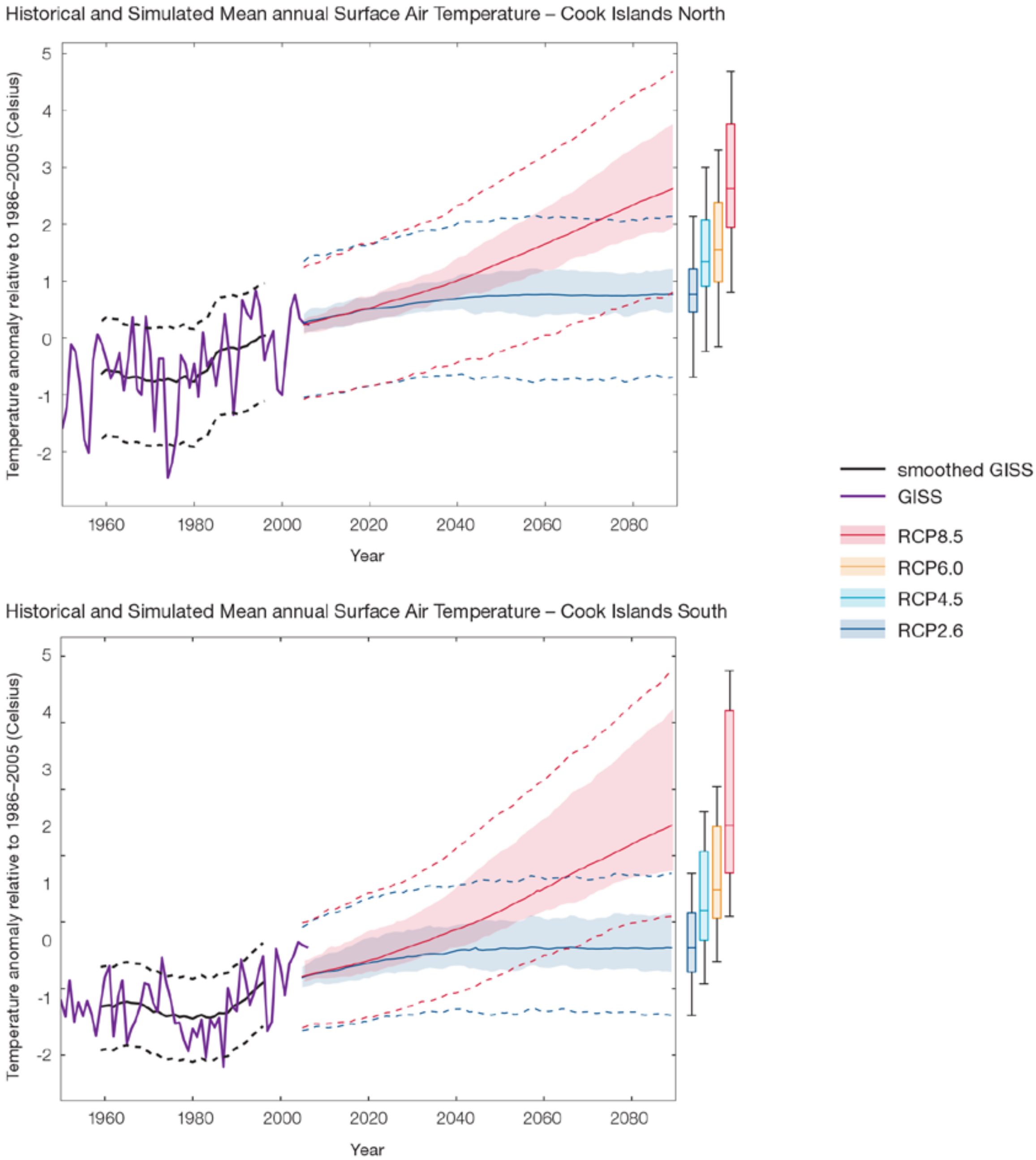

Figure 2.8: Historical and simulated surface air temperature time series for the region surrounding the Northern Cook Islands (top) and the Southern Cook Islands (bottom).The graph shows the anomaly (from the base period 1986–2005) in surface air temperature from observations (the GISS dataset, in purple), and for the CMIP5 models under the very high (RCP8.5, in red) and very low (RCP2.6, in blue) emissions scenarios. The solid red and blue lines show the smoothed (20-year running average) multi-model mean anomaly in surface air temperature, while shading represents the spread of model values (5–95th percentile). The dashed lines show the 5–95th percentile of the observed interannual variability for the observed period (in black) and added to the projections as a visual guide (in red and blue). This indicates that future surface air temperature could be above or below the projected long-term averages due to interannual variability. The ranges of projections for a 20-year period centred on 2090 are shown by the bars on the right for RCP8.5, 6.0, 4.5 and 2.6.

2.5.2 Rainfall

The long-term average rainfall is projected by most models to stay approximately the same as the current records for the Northern Cook Islands and the Southern Cook Islands. The multi-model average shows no marked change under each emission scenario, but with a greater range of uncertainty for the higher emission scenario by the end of the century (Figure 2.9, Tables 2.7 and 2.8). There are some differences in the Northern Cook Islands compared to the Southern Cook Islands. The Northern Cook Islands are projected to get drier in the May–October season under the high emission scenario. These results are different to the results from Australian Bureau of Meteorology and CSIRO (2011), which found that annual and seasonal mean rainfall is projected to increase in the Northern Cook Islands and the Southern Cook Islands.

Mean rainfall increased in the Southern Cook Islands between 1979 and 2006 (Figure 2.9, bottom panel), but the models do not project this will continue into the future. This indicates that the recent increase may be caused by natural variability and not caused by global warming. It is also possible that the models do not simulate a key process driving the recent change. However, the recent change is not particularly large (<10%) and the observed record shown is not particularly long (28 years), so it is difficult to determine the significance of this difference, and its cause. The year-to-year rainfall variability over the Cook Islands is much larger than the projected change, even in the highest emission scenario by 2090. There will still be wet and dry years and decades due to natural variability. There may be different changes across the Northern Cook Islands and the Southern Cook Islands through the local climate influence of topography.

There is general agreement between models that average rainfall will not change significantly from the present day. However, there is a greater range of change under the high emission scenario, and biases in model rainfall in the region of SPCZ. This lowers the confidence of the projected changes, and makes the amount difficult to determine.

There is *medium confidence* that the long-term rainfall over the Cook Islands will remain approximately the same, with the exception of May–October rainfall in the Northern Cook Islands which decreases, because:

- The model average shows little change, and there is a reasonable agreement between models except for the highest emission scenario. The models consistently place the Cook Islands between regions of increasing and decreasing rainfall; and
- Changes in the SPCZ rainfall are uncertain. The majority of CMIP5 models simulate increased rainfall in the western part of the SPCZ (Brown et al., 2013a) and decreased rainfall in the eastern part of the SPCZ, however rainfall changes are sensitive to sea-surface temperature gradients, which are not well simulated in many models (Widlansky et al., 2013). See Box in Chapter 1 for more details.

There is *low confidence* in the multi-model average rainfall change shown in Tables 2.7 and 2.8 because:

- The complex set of processes involved in tropical rainfall is challenging to simulate in models. This means that the confidence in the projection of rainfall is generally lower than for other variables such as temperature;
- There is a different magnitude of change in the SPCZ rainfall projected by models that have reduced sea-surface temperature biases (Australian Bureau of Meteorology and CSIRO, 2011, Chapter 7 (downscaling); Widlanksy et al., 2012) compared to the CMIP5 models; and
- The future behaviour of the ENSO is unclear, and the ENSO strongly influences year-to-year rainfall variability.

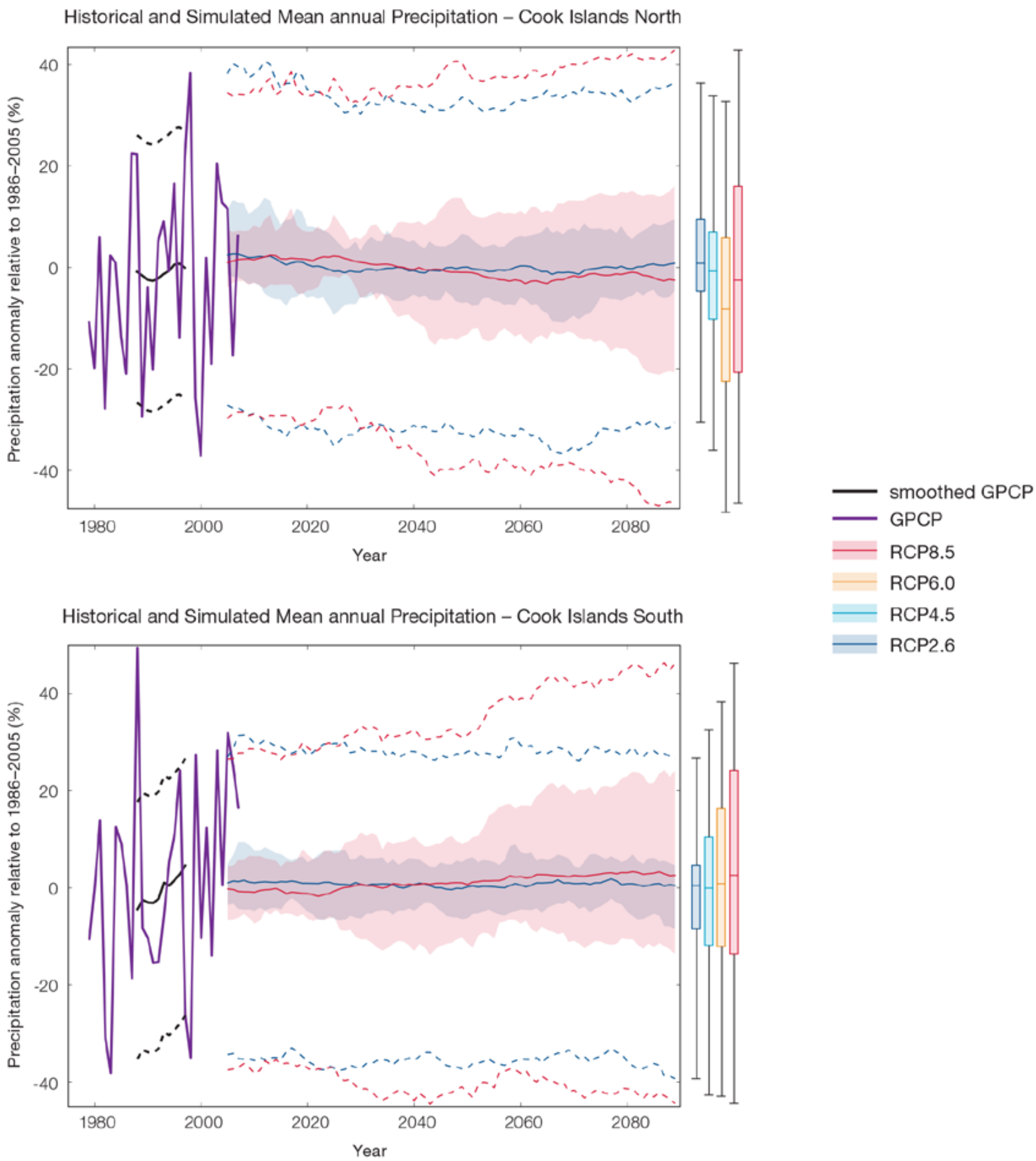

Figure 2.9: Historical and simulated annual average rainfall time series for the region surrounding the Northern Cook Islands (top) and the Southern Cook Islands (bottom).The graph shows the anomaly (from the base period 1986–2005) in rainfall from observations (the GPCP dataset, in purple), and for the CMIP5 models under the very high (RCP8.5, in red) and very low (RCP2.6, in blue) emissions scenarios. The solid red and blue lines show the smoothed (20-year running average) multi-model mean anomaly in rainfall, while shading represents the spread of model values (5–95th percentile). The dashed lines show the 5–95th percentile of the observed interannual variability for the observed period (in black) and added to the projections as a visual guide (in red and blue). This indicates that future rainfall could be above or below the projected long-term averages due to interannual variability. The ranges of projections for a 20-year period centred on 2090 are shown by the bars on the right for RCP8.5, 6.0, 4.5 and 2.6.

2.5.3 Extremes

Extreme Temperature

The temperature on extremely hot days is projected to increase by about the same amount as average temperature. This conclusion is based on analysis of daily temperature data from a subset of CMIP5 models (Chapter 1). The frequency of extremely hot days is also expected to increase.

For the Northern Cook Islands, the temperature of the 1-in-20-year hot day is projected to increase by approximately 0.6°C by 2030 under the RCP2.6 (very low emissions) scenario and by 0.8°C under the RCP8.5 (very high emissions) scenario. By 2090 the projected increase is 0.8°C for RCP2.6 and 2.8°C for RCP8.5.

For the Southern Cook Islands, the temperature of the 1-in-20-year hot day is projected to increase by approximately 0.5°C by 2030 under RCP2.6 scenario and by 0.7°C under RCP8.5 scenario. By 2090 the projected increase is 0.6°C for RCP2.6 and 2.7°C for RCP8.5.

There is *very high confidence* that the temperature of extremely hot days and extremely cool days will increase (Tables 2.7 and 2.8), because:

- A change in the range of temperatures, including the extremes, is physically consistent with rising greenhouse gas concentrations;
- This is consistent with observed increases in extreme temperatures around the world over recent decades; and
- All the CMIP5 models agree on an increase in the frequency and intensity of extremely hot days and a decrease in the frequency and intensity of cool days.

There is *medium confidence* in the magnitude of projected change in extreme temperature because models generally underestimate the current intensity and frequency of extreme events. Changes to the particular driver of extreme temperatures affect whether the change to extremes is more or less than the change in the average temperature, and the changes to the drivers of extreme temperatures in the Cook Islands are currently unclear.

Extreme Rainfall

The frequency and intensity of extreme rainfall events are projected to increase. This conclusion is based on analysis of daily rainfall data from a subset of CMIP5 models using a similar method to that in Australian Bureau of Meteorology and CSIRO (2011) with some improvements (Chapter 1), so the results are slightly different to those in Australian Bureau of Meteorology and CSIRO (2011).

For the Northern Cook Islands, the current 1-in-20-year daily rainfall amount is projected to increase by approximately 3 mm by 2030 for RCP2.6 (very low emissions) and by 7 mm by 2030 for RCP8.5 (very high emissions). By 2090, it is projected to increase by approximately 6 mm for RCP2.6 and by 32 mm for RCP8.5. The majority of models project the current 1-in-20-year daily rainfall event will become, on average, a 1-in-9-year event for RCP2.6 and a 1-in-5-year event for RCP8.5 by 2090.

For the Southern Cook Islands, the current 1-in-20-year daily rainfall amount is projected to increase by approximately 7 mm by 2030 for RCP2.6 and by 9 mm by 2030 for RCP8.5. By 2090, it is projected to increase by approximately 5 mm for RCP2.6 and by 36 mm for RCP8.5. The majority of models project the current 1-in-20-year daily rainfall event will become, on average, a 1-in-9-year event for RCP2.6 and a 1-in-5-year event for RCP8.5 by 2090.

These results are different to those found in Australian Bureau of Meteorology and CSIRO (2011) because of different methods used (Chapter 1).

There is *high confidence* that the frequency and intensity of extreme rainfall events will increase because:

- A warmer atmosphere can hold more moisture, so there is greater potential for extreme rainfall (IPCC, 2012);
- Increases in extreme rainfall in the Pacific are projected in all available climate models; and
- An increase in extreme rainfall events within the South Pacific Convergence Zone (SPCZ) region was found by an in-depth study of extreme rainfall events in the SPCZ (Cai et al., 2012).

There is *low confidence* in the magnitude of projected change in extreme rainfall because:

- Models generally underestimate the current intensity of local extreme events. The simulation of extreme events in the Cook Islands is influenced by the SPCZ biases;
- Changes in extreme rainfall projected by models may be underestimated because models seem to underestimate the observed increase in heavy rainfall with warming (Min et al., 2011);
- GCMs have a coarse spatial resolution, so they do not adequately capture some of the processes involved in extreme rainfall events; and
- The Conformal Cubic Atmospheric Model (CCAM) downscaling model has finer spatial resolution and the CCAM results presented in Australian Bureau of Meteorology and CSIRO (2011) indicates a smaller increase in the number of extreme rainfall days, and there is no clear reason to accept one set of models over another.

Drought

Meteorological drought projections (defined in Chapter 1) are described in terms of changes in proportion of time in drought, frequency and duration by 2090 for RCP2.6 and 8.5.

For the Northern Cook Islands the overall proportion of time spent in drought is expected to increase slightly under RCP8.5 and stay approximately the same under all other scenarios (Figure 2.10). Under RCP8.5 the frequency of extreme droughts is projected to increase while the frequency of events in other categories is projected to decrease slightly. The duration of events is projected to stay approximately the same in all categories under RCP8.5. Under RCP2.6 the frequency and duration of events in all drought categories is projected to stay approximately the same from the present to 2090.

For the Southern Cook Islands the overall proportion of time spent in drought is expected to decrease slightly under RCP8.5 and stay approximately the same under all other scenarios (Figure 2.10). Under RCP8.5 the frequency of mild droughts is projected to decrease while the frequency of events in other categories is projected to remain the same. The duration of events is projected to stay approximately the same in all categories under RCP8.5. Under RCP2.6 the frequency and duration of events in all drought categories is projected to stay approximately the same from the present to 2090.

These results are different from those found in Australian Bureau of Meteorology and CSIRO (2011), which reported that the incidence of drought is projected to decrease in the Northern and Southern Cook Islands.

There is *medium confidence* in this direction of change because:

- There is only *medium confidence* in the direction of mean rainfall change;
- These drought projections are based upon a subset of models; and
- Like the CMIP3 models, the majority of the CMIP5 models agree on this direction of change.

There is *low confidence* in the projections of drought frequency and duration because there is *low confidence* in the magnitude of rainfall projections, and no consensus about projected changes in the El Niño–Southern Oscillation, which directly influence the projection of drought.

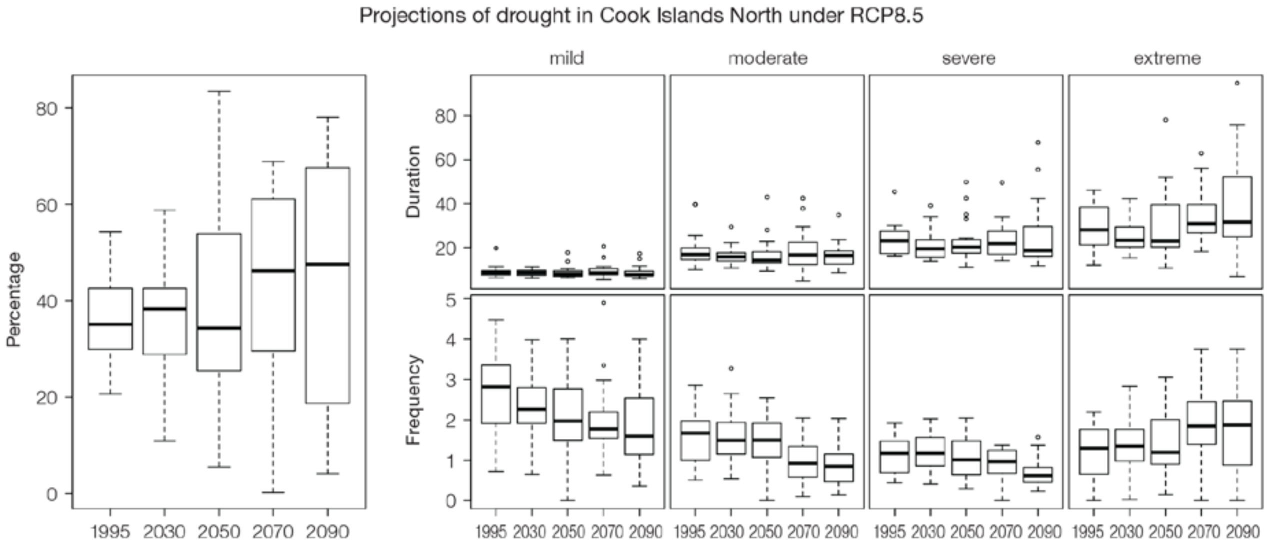

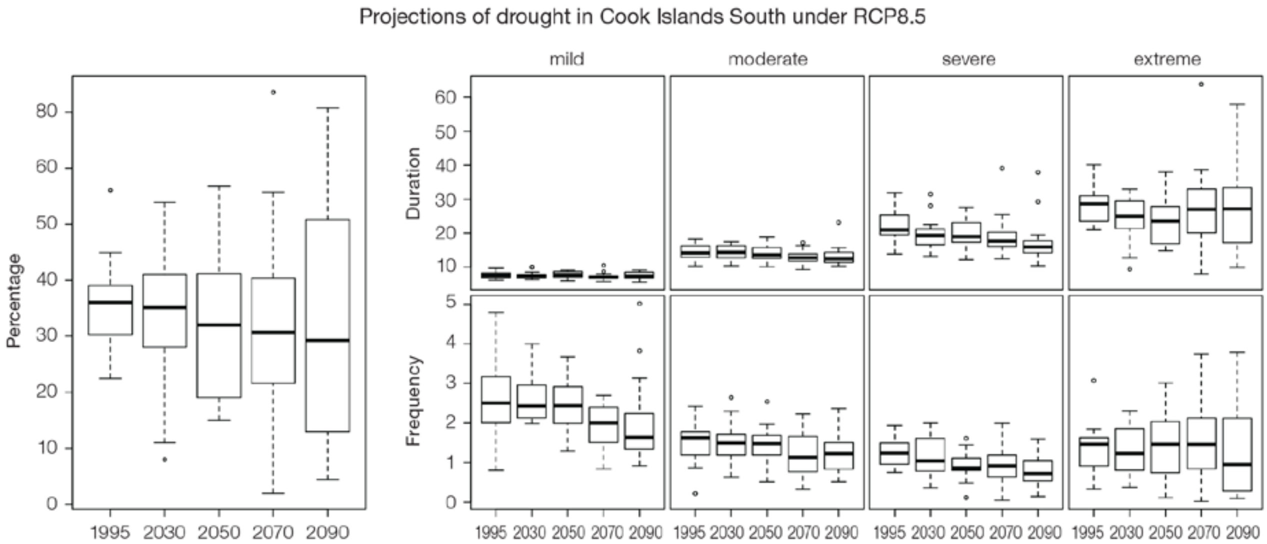

Figure 2.10: Box-plots showing percent of time in moderate, severe or extreme drought (left hand side), and average drought duration and frequency for the different categories of drought (mild, moderate, severe and extreme) for the Northern Cook Islands (top) and Southern Cook Islands (bottom). These are shown for 20-year periods centred on 1995, 2030, 2050, 2070 and 2090 for the RCP8.5 (very high emissions) scenario. The thick dark lines show the median of all models, the box shows the interquartile (25–75%) range, the dashed lines show 1.5 times the interquartile range and circles show outlier results.

Tropical Cyclones

Global Picture

There is a growing level of consistency between models that on a global basis the frequency of tropical cyclones is likely to decrease by the end of the 21st century. The magnitude of the decrease varies from 6%–35% depending on the modelling study. There is also a general agreement between models that there will be an increase in the mean maximum wind speed of cyclones by between 2% and 11% globally, and an increase in rainfall rates of the order of 20% within 100 km of the cyclone centre (Knutson et al., 2010). Thus, the scientific community has a *medium* level of confidence in these global projections.

Cook Islands

In the Cook Islands, the projection is for a decrease in cyclone genesis (formation) frequency for the South-east basin (see Figure 2.11 and Table 2.4). The confidence level for this projection is high. The GCMs show consistent results across models for changes in cyclone frequency for the South-east basin, using the direct detection methodologies described in Chapter 1. Approximately 80% of the projected changes, based on these methods, vary between a 5% decrease to a 50% decrease in genesis frequency with half projecting a decrease between 20 and 40%. Projections based upon empirical techniques suggest the conditions for cyclone formation will become less favourable in this region with about half of projected changes indicating decreases between 10 and 40% in genesis frequency. These projections are consistent with those of Australian Bureau of Meteorology and CSIRO (2011).

Table 2.4: Projected percentage change in cyclone frequency in the south-east basin (0–40°S; 170°E–130°W), for 2080–2099 relative to 1980–1999 for RCP8.5 (very high emissions) and based on five methods. 22 CMIP5 climate models were selected based upon the availability of data or on their ability to reproduce a current-climate tropical cyclone climatology (See Section 1.5.3 – Detailed Projection Methods, Tropical Cyclones). Blue numbers indicate projected decreases in tropical cyclone frequency, red numbers an increase. MMM is the multi-model mean change. N increase is the proportion of models (for the individual projection method) projecting an increase in cyclone formation.

Model	GPI change	GPI-M change	Tippett	CDD	OWZ
access10	5	-22	-54	-23	
access13	-26	-26	-36	-10	
bcccsm11	-3	-1	-28		-5
canesm2	-7	-13	-49	-6	
ccsm4				-78	-5
cnrm_cm5	-4	-5	-26	8	7
csiro_mk36	-16	-13	-33	-26	-27
fgoals_g2	6	-8	-40		
fgoals_s2	-15	-20	-48		
gfdl_esm2m				-48	-36
gfdl_cm3	-1	-5	-25		-11
gfdl_esm2g				-18	-36
gisse2r	17	16	-6		
hadgem2_es	-8	-11	-51		
inm	-3	-3	-30		
ipslcm5alr	-13	-19	-43		
ipslcm5blr				7	
miroc5				-43	-22
mirocesm	-40	-38	46		
mpim	-26	-19	-41		
mricgcm3	-8	-10	-28		
noresm1m	-36	-40	-59	-80	
MMM	-11	-14	-32	-29	-17
N increase	0.2	0.1	0.1	0.2	0.125

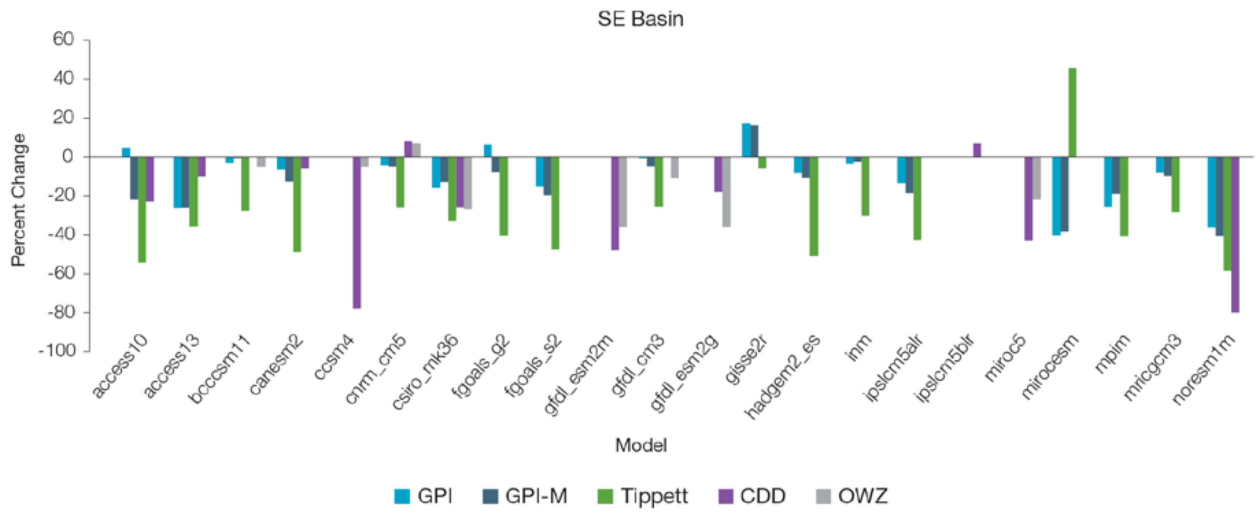

Figure 2.11: Projected percentage change in cyclone frequency in the south-east basin (data from Table 2.4).

2.5.4 Coral Reefs and Ocean Acidification

As atmospheric CO_2 concentrations continue to rise, oceans will warm and continue to acidify. These changes will affect the health and viability of marine ecosystems, including coral reefs that provide many key ecosystem services, such as food, resources for livelihoods (e.g. tourism) and coastal protection (*high confidence*). These impacts are also likely to be compounded by other stressors such as storm damage, fishing pressure and other human impacts.

The projections for future ocean acidification and coral bleaching use three RCPs (2.6, 4.5, and 8.5).

Ocean acidification

Ocean acidification is expressed in terms of aragonite saturation state (Chapter 1). In the Northern Cook Islands and the Southern Cook Islands, the aragonite saturation state has declined from about 4.5 in the late 18th century to an observed value of about 4.1±0.2 in 2000 (Kuchinke et al., 2014). All models show that the aragonite saturation state, a proxy for coral reef growth rate, will continue to decrease as atmospheric CO_2 concentrations increase (*very high confidence*). Projections from CMIP5 models indicate that under RCP8.5 and RCP4.5 the median aragonite saturation state will transition to marginal conditions (3.5) around 2030. In RCP8.5 the aragonite saturation state continues to strongly decline thereafter to values where coral reefs have not historically been found (< 3.0). Under RCP4.5 (low emissions) the aragonite saturation plateaus around 3.2, i.e. marginal conditions for healthy coral reefs. Under RCP2.6, the median aragonite saturation state never falls below 3.5, and increases slightly toward the end of the century (Figure 2.12), suggesting that the conditions remain adequate for healthy corals reefs. There is *medium confidence* in this range and distribution of possible futures because the projections are based on climate models that do not resolve the reef scale that can play a role in modulating large-scale changes. The impacts of ocean acidification are also likely to affect the entire marine ecosystem, affecting the key ecosystem services provided by reefs.

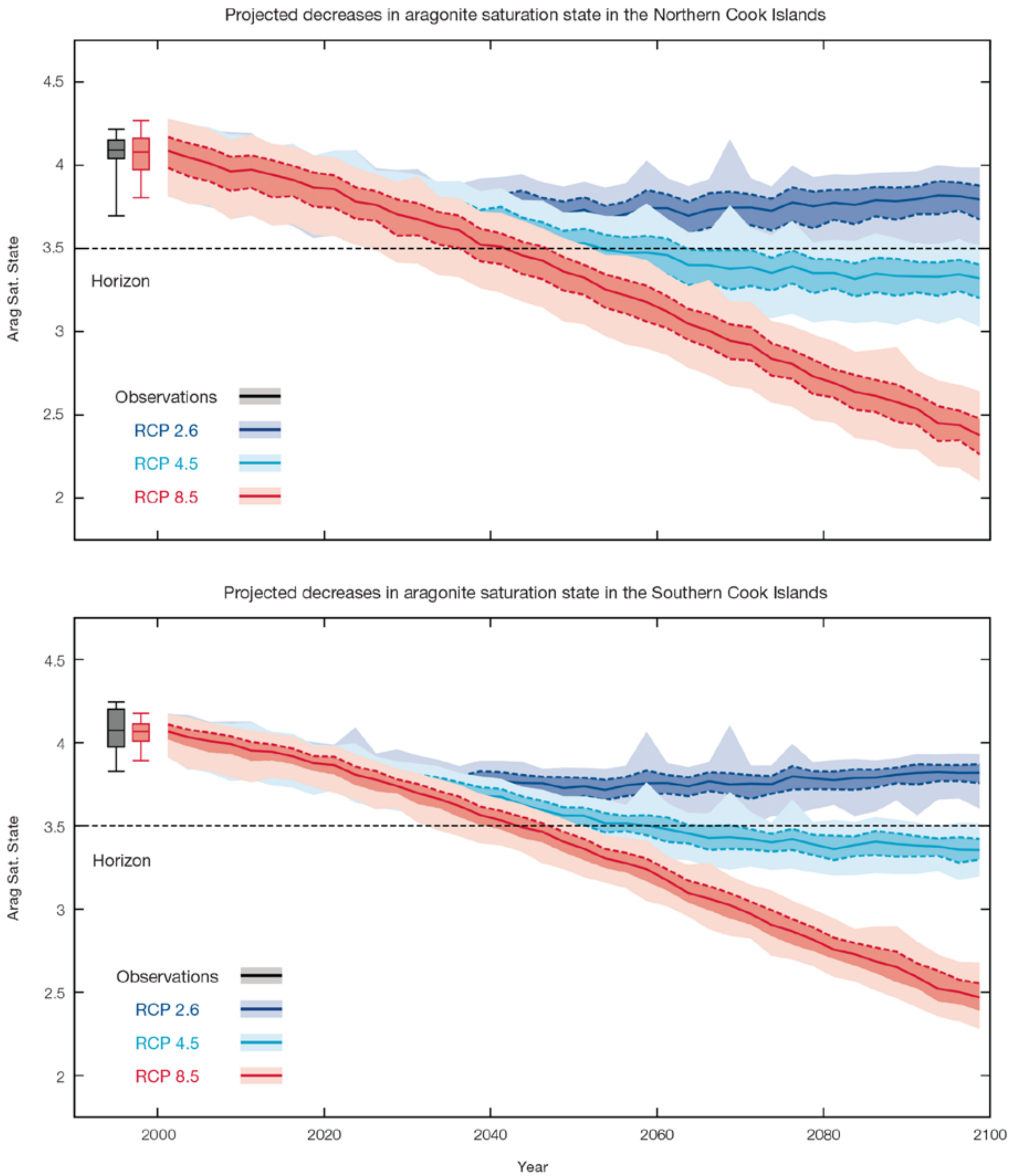

Figure 2.12: Projected decreases in aragonite saturation state in the Northern (top) and Southern (bottom) Cook Islands from CMIP5 models under RCP2.6, 4.5 and 8.5. Shown are the median values (solid lines), the interquartile range (dashed lines), and 5% and 95% percentiles (light shading). The horizontal line represents the transition to marginal conditions for coral reef health (from Guinotte et al., 2003).

Coral Bleaching Risk

As the ocean warms, the risk of coral bleaching increases (*very high confidence*). There is *medium confidence* in the projected increase in coral bleaching risk for the Cook Islands because there is *medium confidence* in the rate of increase of sea-surface temperature (SST), and the changes at the reef scale (which can play a role in modulating large-scale changes) are not adequately simulated. Importantly, the coral bleaching risk calculation does not account the impact of other potential stressors (Chapter 1).

The changes in the frequency (or recurrence) and duration of severe bleaching risk are quantified for different projected SST changes (Table 2.5 – Northern Cook Islands and Table 2.6 – Southern Cook Islands). Overall there is a decrease in the time between two periods of elevated risk and an increase in the duration of the elevated risk. For example, under a long-term mean increase of 1°C (relative to 1982–1999 period), the average period of severe bleaching risk (referred to as a risk event) will last 10.6 weeks (with a minimum duration of 2.5 weeks and a maximum duration of 3.8 months) and the average time between two periods of elevated risk will be 2.7 years (with the minimum recurrence of 5.2 months and a maximum recurrence of 7.5 years). If severe bleaching events occur more often than once every five years, the long-term viability of coral reef ecosystems becomes threatened.

Table 2.5: Projected changes in severe coral bleaching risk for the Northern Cook Islands EEZ for increases in SST relative to 1982–1999.

Temperature change [1]	Recurrence interval [2]	Duration of the risk event [3]
Change in observed mean	0	0
+0.25°C	30 years	4 weeks
+0.5°C	28.2 years (27.4 years – 29.9 years)	4.7 weeks (4.5 weeks – 4.9 months)
+0.75°C	6.6 years (1.6 years – 14.4 years)	6.7 weeks (3.3 weeks – 9.8 months)
+1°C	2.7 years (5.2 months – 7.5 years)	10.6 weeks (2.5 weeks – 3.8 months)
+1.5°C	10.9 months (2.1 months – 2.7 years)	3.6 months (2.9 weeks – 6.3 months)
+2°C	6.5 months (1.8 months – 1.4 years)	6.0 months (6.1 weeks – 8.2 months)

[1] This refers to projected SST anomalies above the mean for 1982–1999.
[2] Recurrence is the mean time between severe coral bleaching risk events. Range (min – max) shown in brackets.
[3] Duration refers to the period of time where coral are exposed to the risk of severe bleaching. Range (min – max) shown in brackets.

Table 2.6: Projected changes in severe coral bleaching risk for the Southern Cook Islands EEZ for increases in SST relative to 1982–1999.

Temperature change [1]	Recurrence interval [2]	Duration of the risk event [3]
Change in observed mean	0	0
+0.25°C	30 years	2 weeks
+0.5°C	28.2 years (27.9 years – 28.6 years)	6.0 weeks (5.8 weeks – 1.4 months)
+0.75°C	10.7 years (7.0 years – 14.4 years)	6.9 weeks (4.6 weeks – 2.1 months)
+1°C	3.4 years (11.8 months – 7.0 years)	8.8 weeks (3.5 weeks – 2.8 months)
+1.5°C	1.1 years (5.5 months – 2.4 years)	3.0 months (4.3 weeks – 5.0 months)
+2°C	8.5 months (5.5 months – 1.6 years)	4.4 months (6.6 weeks – 6.7 months)

[1] This refers to projected SST anomalies above the mean for 1982–1999.
[2] Recurrence is the mean time between severe coral bleaching risk events. Range (min – max) is shown in brackets.
[3] Duration refers to the period of time where coral are exposed to the risk of severe bleaching. Range (min – max) is shown in brackets.

2.5.5 Sea Level

Mean sea level is projected to continue to rise over the course of the 21st century. There is very *high confidence* in the direction of change. The CMIP5 models simulate a rise of between approximately 7–17 cm by 2030 (very similar values for different RCPs), with increases of 39–86 cm by 2090 under the RCP8.5 (Figure 2.13 and Table 2.7). There is *medium confidence* in the range mainly because there is still uncertainty associated with projections of the Antarctic ice sheet contribution. Interannual variability of sea level will lead to periods of lower and higher regional sea levels. In the past, this interannual variability has been about 19 cm (5–95% range, after removal of the seasonal signal, see dashed lines in Figure 2.13 (a) and it is likely that a similar range will continue through the 21st century.

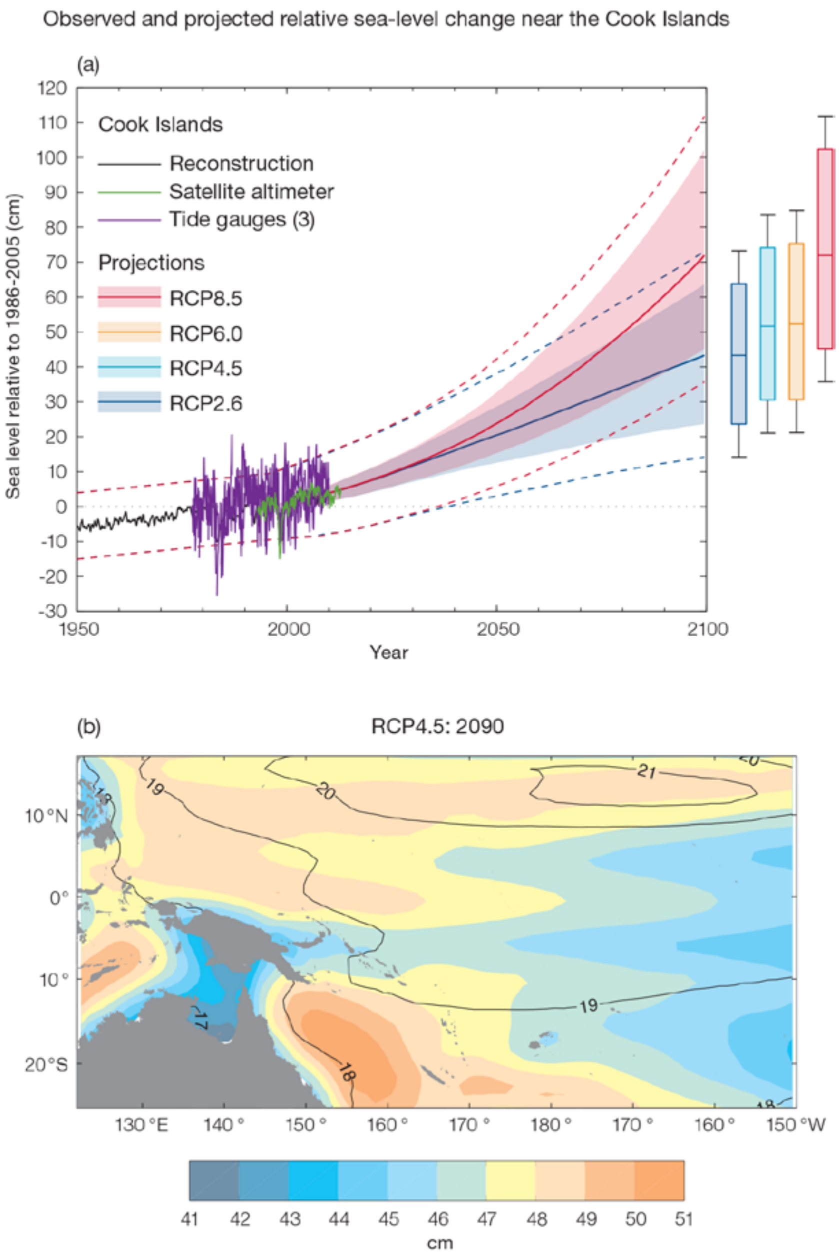

Figure 2.13 (a): The observed tide-gauge records of relative sea-level (since the late 1970s) are indicated in purple, and the satellite record (since 1993) in green. The gridded (reconstructed) sea level data at the Cook Islands (since 1950) is shown in black. Multi-model mean projections from 1995–2100 are given for the RCP8.5 (red solid line) and RCP2.6 emissions scenarios (blue solid line), with the 5–95% uncertainty range shown by the red and blue shaded regions. The ranges of projections for four emission scenarios (RCPs 2.6, 4.5, 6.0 and 8.5) by 2100 are also shown by the bars on the right. The dashed lines are an estimate of interannual variability in sea level (5–95% uncertainty range about the projections) and indicate that individual monthly averages of sea level can be above or below longer-term averages.

(b) The regional distribution of projected sea level rise under the RCP4.5 emissions scenario for 2081–2100 relative to 1986–2005. Mean projected changes are indicated by the shading, and the estimated uncertainty in the projections is indicated by the contours (in cm).

2.5.6 Wind-driven Waves

The projected changes in wave climate vary across the Cook Islands.

In the Northern Cook Islands, projected changes in wave properties include a small and largely non-significant decrease in wave height in November to March (Figure 2.14) with no change in wave period or direction during December–March (*low confidence*) (Table 2.9). During June–September, wave height is projected to increase in September, otherwise no significant changes are projected to occur in wave climate (*low confidence*), with less variable wave directions. An increase in the height of storm waves is indicated in December–March (*low confidence*).

In the Southern Cook Islands, there is a projected small decrease in December–March wave height and period (significant in January under RCP8.5 (very high emissions) by 2090 (Figure 2.15) with no change in direction (*low confidence*) (Table 2.10). In June–September, there is no projected change in wave height or period but a small anticlockwise rotation toward the east is simulated (*low confidence*). No change is projected in storm waves (*low confidence*).

There is *low confidence* in projected changes in the Cook Islands wind-wave climate because:

- Projected changes in wave climate are dependent on confidence in projected changes in the El Niño–Southern Oscillation, which is low.
- The differences between simulated and observed (hindcast) wave data are larger than the projected wave changes, which further reduces our confidence in projections.

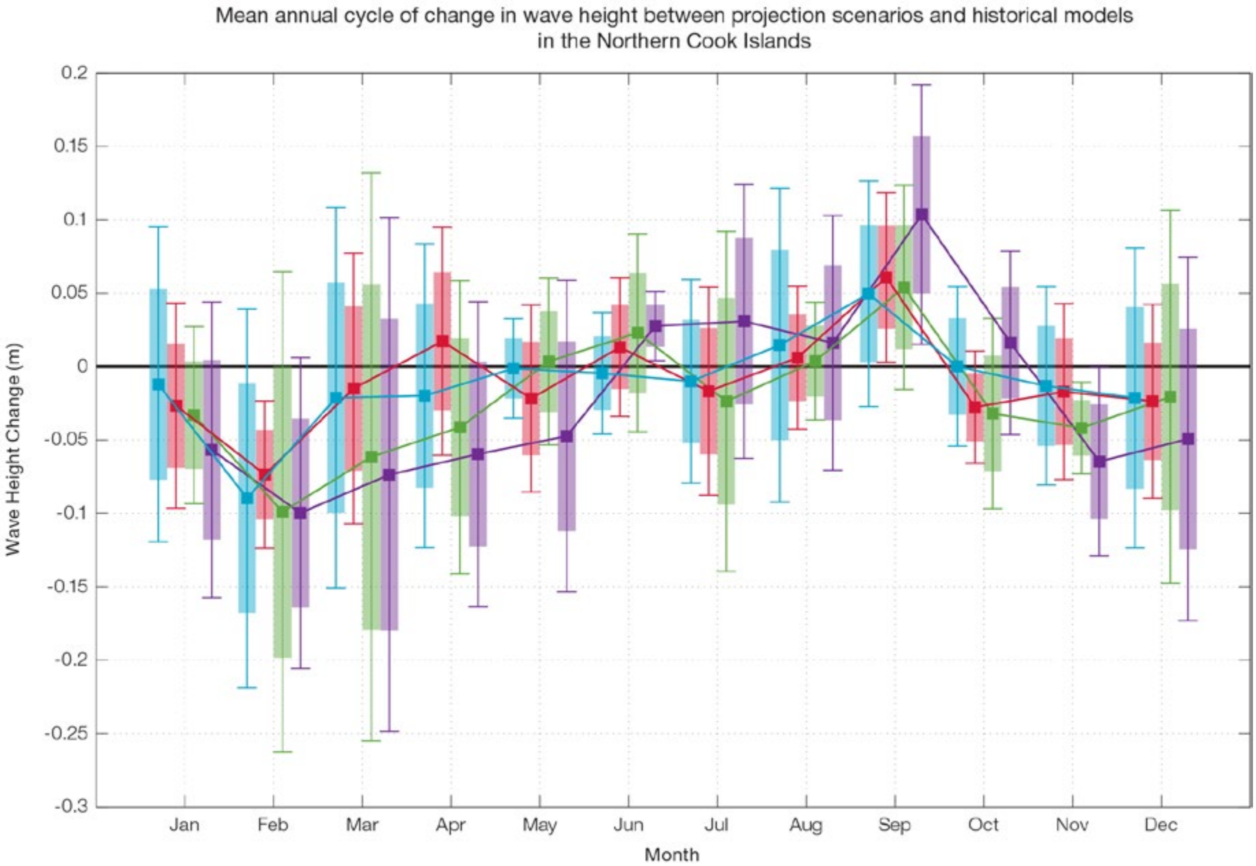

Figure 2.14: Mean annual cycle of change in wave height (m) between projection scenarios and historical models in the Northern Cook Islands. Shaded boxes show 1 standard deviation of models' means around the ensemble means, and error bars show the 5–95% range inferred from the standard deviation. Colours represent RCP scenarios and time periods: blue 2035 RCP4.5 (low emissions), red 2035 RCP8.5 (very high emissions), green 2090 RCP4.5 (low emissions), purple 2090 RCP8.5 (very high emissions).

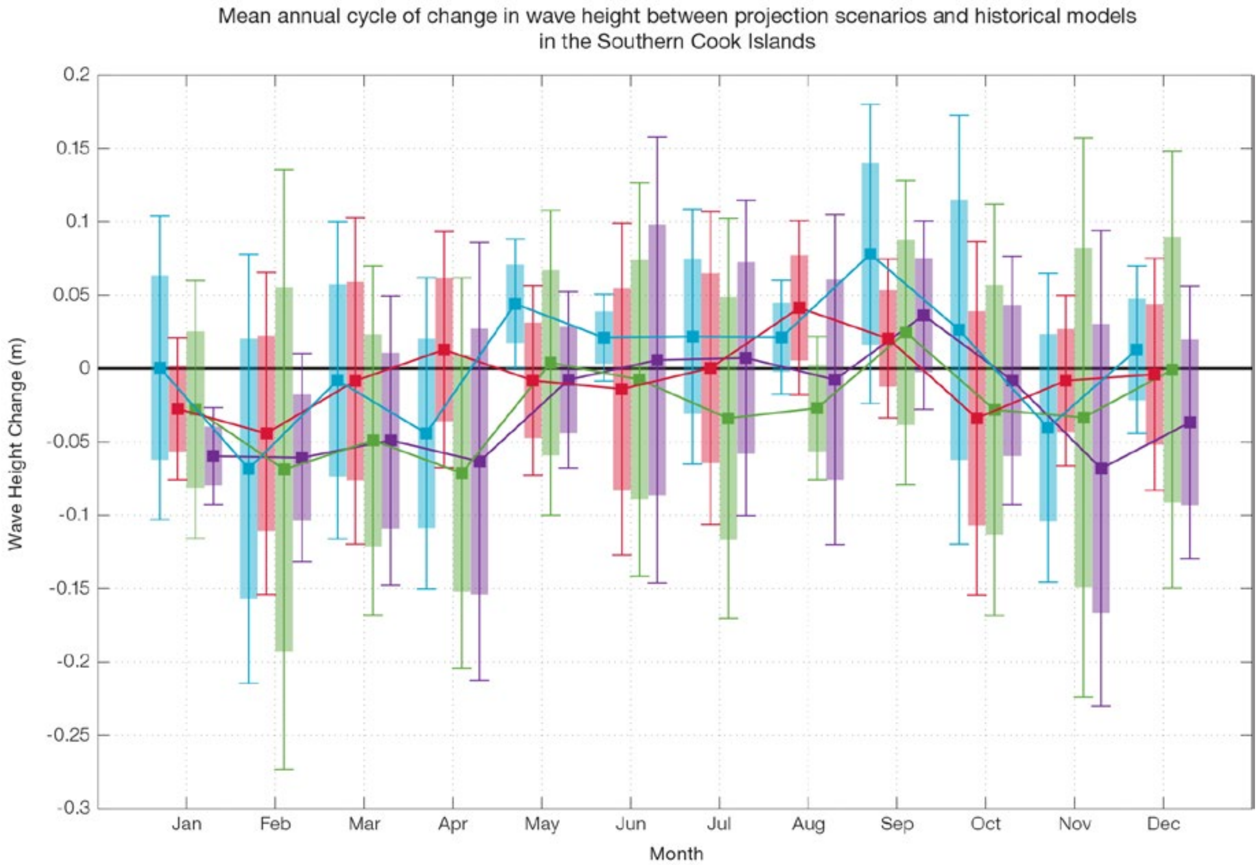

Figure 2.15: Mean annual cycle of change in wave height (m) between projection scenarios and historical models in the Southern Cook Islands. Shaded boxes show 1 standard deviation of models' means around the ensemble means, and error bars show the 5–95% range inferred from the standard deviation. Colours represent RCP scenarios and time periods: blue 2035 RCP4.5 (low emissions), red 2035 RCP8.5 (very high emissions), green 2090 RCP4.5 (low emissions), purple 2090 RCP8.5 (very high emissions).

2.5.7 Projections Summary

There is *very high confidence* in the direction of long-term change in a number of key climate variables, namely an increase in mean and extremely high temperatures, sea level and ocean acidification. There is *high confidence* that the frequency and intensity of extreme rainfall will increase. There is *medium confidence* that mean rainfall and drought frequency will stay approximately the same, except for the Northern Cook Islands in the May–October season which is projected to get drier.

Tables 2.7–2.10 quantify the mean changes and ranges of uncertainty for a number of variables, years and emissions scenarios. A number of factors are considered in assessing confidence, i.e. the type, amount, quality and consistency of evidence (e.g. mechanistic understanding, theory, data, models, expert judgment) and the degree of model agreement, following the IPCC Guidelines (Mastrandrea et al., 2010). Confidence ratings in the projected magnitude of mean change are generally lower those for the direction of change (see paragraph above) because magnitude of change is more difficult to assess. For example, there is *very high confidence* that temperature will increase, but *medium confidence* in the magnitude of mean change.

Table 2.7: Projected changes in the annual and seasonal mean climate for the Northern Cook Islands under four emissions scenarios; RCP2.6 (very low emissions, in dark blue), RCP4.5 (low emissions, in light blue), RCP6 (medium emissions, in orange) and RCP8.5 (very high emissions, in red). Projected changes are given for four 20-year periods centred on 2030, 2050, 2070 and 2090, relative to a 20-year period centred on 1995. Values represent the multi-model mean change, with the 5–95% range of uncertainty in brackets. Confidence in the magnitude of change is expressed as *high*, *medium* or *low*. Surface air temperatures in the Pacific are closely related to sea-surface temperatures (SST), so the projected changes to air temperature given in this table can be used as a guide to the expected changes to SST. (See also Section 1.5.2). 'NA' indicates where data are not available.

Variable	Season	2030	2050	2070	2090	Confidence (magnitude of change)
Surface air temperature (°C)	Annual	0.6 (0.4–0.9)	0.7 (0.5–1.2)	0.8 (0.4–1.2)	0.8 (0.5–1.2)	*High*
		0.7 (0.4–1)	1 (0.6–1.3)	1.2 (0.8–1.8)	1.3 (0.9–2.1)	
		0.6 (0.4–0.9)	0.9 (0.6–1.4)	1.2 (0.8–1.8)	1.6 (1–2.4)	
		0.8 (0.5–1)	1.3 (0.9–1.8)	2 (1.5–2.9)	2.7 (2–3.8)	
Maximum temperature (°C)	1-in-20 year event	0.6 (0.1–0.8)	0.8 (0.1–1.2)	0.8 (0–1.4)	0.8 (0.2–1.1)	*Medium*
		0.6 (0.2–0.8)	0.9 (0.4–1.2)	1.1 (0.1–1.7)	1.3 (0.6–1.9)	
		NA (NA–NA)	NA (NA–NA)	NA (NA–NA)	NA (NA–NA)	
		0.7 (0.2–1.1)	1.4 (0.5–2.1)	2.2 (0.8–3.1)	2.8 (1.3–4.2)	
Minimum temperature (°C)	1-in-20 year event	0.6 (0.3–1)	0.7 (0–1.1)	0.8 (0.2–1.2)	0.8 (0.2–1.1)	*Medium*
		0.6 (0.2–0.9)	0.9 (0.5–1.3)	1.1 (0.7–1.7)	1.3 (0.6–2)	
		NA (NA–NA)	NA (NA–NA)	NA (NA–NA)	NA (NA–NA)	
		0.8 (0.4–1.1)	1.4 (0.9–2)	2.1 (1.5–2.9)	2.8 (1.9–4)	
Total rainfall (%)	Annual	-1 (-7–5)	0 (-7–7)	-1 (-10–7)	1 (-5–9)	*Low*
		1 (-6–9)	1 (-7–9)	0 (-8–9)	-1 (-10–7)	
		-1 (-8–6)	-3 (-7–1)	-5 (-15–4)	-8 (-22–6)	
		1 (-4–6)	-1 (-14–14)	-2 (-13–13)	-3 (-21–16)	
Total rainfall (%)	Nov-Apr	1 (-4–8)	2 (-5–10)	2 (-7–9)	3 (-3–16)	*Low*
		3 (-5–9)	2 (-7–13)	3 (-8–10)	2 (-5–9)	
		0 (-7–10)	-2 (-7–3)	-3 (-15–7)	-3 (-21–9)	
		3 (-5–7)	2 (-11–12)	3 (-10–14)	3 (-20–22)	
Total rainfall (%)	May-Oct	-4 (-12–4)	-3 (-16–5)	-5 (-16–6)	-3 (-10–6)	*Low*
		-1 (-9–9)	-2 (-14–12)	-4 (-16–9)	-5 (-20–4)	
		-3 (-12–5)	-6 (-13–0)	-9 (-22–4)	-15 (-30–0)	
		-2 (-11–7)	-5 (-21–16)	-9 (-27–12)	-11 (-35–13)	
Aragonite saturation state (Ωar)	Annual	-0.3 (-0.6–0.0)	-0.4 (-0.7–-0.1)	-0.4 (-0.6–-0.1)	-0.3 (-0.6–0.0)	*Medium*
		-0.3 (-0.6–0.0)	-0.5 (-0.8–-0.2)	-0.7 (-0.9–-0.4)	-0.7 (-1.0–-0.4)	
		NA (NA–NA)	NA (NA–NA)	NA (NA–NA)	NA (NA–NA)	
		-0.4 (-0.7–-0.1)	-0.7 (-1.0–-0.4)	-1.1 (-1.4–-0.8)	-1.5 (-1.7–-1.2)	
Mean sea level (cm)	Annual	12 (7–17)	21 (13–29)	30 (18–43)	39 (22–57)	*Medium*
		12 (7–17)	22 (14–30)	33 (21–47)	46 (28–65)	
		11 (7–16)	21 (13–29)	33 (20–46)	46 (28–66)	
		12 (8–17)	24 (16–33)	40 (26–56)	61 (39–86)	

Table 2.8: Projected changes in the annual and seasonal mean climate for the Southern Cook Islands under four emissions scenarios; RCP2.6 (very low emissions, in dark blue), RCP4.5 (low emissions, in light blue), RCP6 (medium emissions, in orange) and RCP8.5 (very high emissions, in red). Projected changes are given for four 20-year periods centred on 2030, 2050, 2070 and 2090, relative to a 20-year period centred on 1995. Values represent the multi-model mean change, with the 5–95% range of uncertainty in brackets. Confidence in the magnitude of change is expressed as *high*, *medium* or *low*. Surface air temperatures in the Pacific are closely related to sea-surface temperatures (SST), so the projected changes to air temperature given in this table can be used as a guide to the expected changes to SST. (See also Section 1.5.2). 'NA' indicates where data are not available.

Variable	Season	2030	2050	2070	2090	Confidence (magnitude of change)
Surface air temperature (°C)	Annual	0.5 (0.3–0.9)	0.6 (0.3–1)	0.6 (0.3–1.1)	0.6 (0.2–1.1)	*High*
		0.6 (0.3–0.9)	0.9 (0.6–1.5)	1.1 (0.7–1.8)	1.2 (0.7–2.1)	
		0.5 (0.3–0.9)	0.8 (0.5–1.4)	1.1 (0.8–1.9)	1.5 (1.1–2.4)	
		0.6 (0.4–1)	1.2 (0.8–2)	1.8 (1.3–3)	2.5 (1.7–4.2)	
Maximum temperature (°C)	1-in-20 year event	0.5 (0.2–0.8)	0.5 (0–0.9)	0.6 (0.1–1.1)	0.6 (0.1–1.1)	*Medium*
		0.5 (0.2–0.8)	0.8 (0.3–1.2)	1.1 (0.5–1.6)	1.2 (0.7–1.8)	
		NA (NA–NA)	NA (NA–NA)	NA (NA–NA)	NA (NA–NA)	
		0.7 (0.2–1.1)	1.3 (0.9–1.8)	2 (1.1–2.8)	2.7 (1.6–3.9)	
Minimum temperature (°C)	1-in-20 year event	0.5 (0.1–0.7)	0.6 (-0.1–1)	0.6 (-0.1–0.9)	0.6 (-0.1–1)	*Medium*
		0.4 (0–0.8)	0.8 (0.4–1.4)	1.1 (0.5–1.9)	1.1 (0.6–1.8)	
		NA (NA–NA)	NA (NA–NA)	NA (NA–NA)	NA (NA–NA)	
		0.7 (0.3–1)	1.3 (0.6–1.9)	2 (1.6–3)	2.8 (2–4.5)	
Total rainfall (%)	Annual	1 (-6–6)	0 (-6–5)	1 (-3–6)	0 (-8–5)	*Low*
		1 (-10–9)	2 (-8–11)	4 (-7–15)	0 (-12–10)	
		1 (-5–8)	1 (-8–10)	3 (-9–17)	1 (-12–16)	
		0 (-10–10)	1 (-10–9)	2 (-11–20)	3 (-14–24)	
Total rainfall (%)	Nov-Apr	0 (-9–7)	0 (-9–10)	1 (-7–9)	-1 (-9–7)	*Low*
		1 (-8–8)	2 (-10–17)	3 (-7–17)	1 (-15–18)	
		1 (-7–10)	-1 (-13–11)	1 (-13–19)	0 (-16–20)	
		1 (-10–14)	1 (-9–13)	2 (-13–26)	3 (-18–26)	
Total rainfall (%)	May-Oct	3 (-4–9)	1 (-8–12)	1 (-7–7)	4 (-4–10)	*Low*
		1 (-8–9)	1 (-8–10)	4 (-8–17)	0 (-8–12)	
		1 (-7–8)	5 (-3–12)	7 (-6–21)	3 (-12–19)	
		1 (-4–8)	2 (-12–15)	3 (-7–11)	3 (-15–26)	
Aragonite saturation state (Ωar)	Annual	-0.3 (-0.6–-0.1)	-0.4 (-0.7–-0.1)	-0.4 (-0.7–-0.1)	-0.3 (-0.6–0.0)	*Medium*
		-0.4 (-0.6–-0.1)	-0.6 (-0.8–-0.3)	-0.7 (-1.0–-0.4)	-0.8 (-1.0–-0.5)	
		NA (NA–NA)	NA (NA–NA)	NA (NA–NA)	NA (NA–NA)	
		-0.4 (-0.7–-0.1)	-0.8 (-1.0–-0.5)	-1.1 (-1.4–-0.9)	-1.5 (-1.8–-1.3)	
Mean sea level (cm)	Annual	12 (7–17)	21 (13–29)	30 (18–43)	39 (22–57)	*Medium*
		12 (7–17)	22 (14–30)	33 (21–47)	46 (28–65)	
		11 (7–16)	21 (13–29)	33 (20–46)	46 (28–66)	
		12 (8–17)	24 (16–33)	40 (26–56)	61 (39–86)	

Waves Projections Summary

Table 2.9: Projected average changes in wave height, period and direction in the Northern Cook Islands for December–March and June–September for RCP4.5 (low emissions, in blue) and RCP8.5 (very high emissions, in red), for two 20-year periods (2026–2045 and 2081–2100), relative to a 1986–2005 historical period. The values in brackets represent the 5th to 95th percentile range of uncertainty.

Variable	Season	2035	2090	Confidence (range)
Wave height change (m)	December–March	-0.0 (-0.3–0.2) -0.0 (-0.3–0.2)	-0.1 (-0.3–0.2) -0.1 (-0.3–0.2)	*Low*
	June–September	0.0 (-0.2–0.2) +0.0 (-0.1–0.2)	0.0 (-0.1–0.2) +0.0 (-0.2–0.3)	*Low*
Wave period change (s)	December–March	+0.0 (-1.7–1.8) -0.0 (-1.7–1.6)	-0.1 (-2.0–1.9) -0.1 (-2.2–2.0)	*Low*
	June–September	+0.0 (-1.1–1.2) +0.0 (-1.1 to1.1)	-0.0 (-1.3–1.2) -0.0 (-1.4–1.3)	*Low*
Wave direction change (° clockwise)	December–March	+0 (-30–40) 0 (-30–30)	0 (-30–30) 0 (-40–40)	*Low*
	June–September	0 (-10–10) 0 (-10–10)	-0 (-20–10) -0 (-20–10)	*Low*

Table 2.10: Projected average changes in wave height, period and direction in the Southern Cook Islands for December–March and June–September for RCP4.5 (low emissions, in blue) and RCP8.5 (very high emissions, in red), for two 20-year periods (2026–2045 and 2081–2100), relative to a 1986–2005 historical period. The values in brackets represent the 5th to 95th percentile range of uncertainty.

Variable	Season	2035	2090	Confidence (range)
Wave height change (m)	December–March	0.0 (-0.3–0.2) -0.0 (-0.3–0.2)	-0.0 (-0.3–0.2) -0.1 (-0.3–0.2)	*Low*
	June–September	+0.0 (-0.3–0.4) 0.0 (-0.3–0.3)	0.0 (-0.4–0.4) 0.0 (-0.4–0.4)	*Low*
Wave period change (s)	December–March	-0.0 (-1.5–1.4) -0.0 (-1.4—1.3)	-0.1 (-1.7–1.5) -0.1 (-1.9–1.6)	*Low*
	June–September	0.0 (-0.9–0.9) 0.0 (-0.9–0.9)	0.0 (-1.1–1.1) -0.0 (-1.2–1.1)	*Low*
Wave direction change (° clockwise)	December–March	0 (-70–70) 0 (-60–60)	-0 (-60–60) -10 (-70–60)	*Low*
	June–September	-0 (-20–10) -0 (-20–10)	-0 (-20–10) -10 (-20–5)	*Low*

Wind-wave variables parameters are calculated for a 20-year period centred on 2035.